INVESTIGATING THE FORMATION AND STRUCTURE OF MERCURY'S CALORIS IMPACT BASIN

Ross W. K. Potter[1,2] and James W. Head[1,2], [1]Department of Earth, Environmental and Planetary Sciences, Brown University, Providence, RI, 02912, USA, [2]NASA Solar System Exploration Research Virtual Institute, ross_potter@brown.edu.

Introduction: With a diameter of ~1500 km [1,2], Caloris is the largest impact basin on Mercury and one of the largest within the Solar System. Caloris, formed ~3.9 Ga [3], is also the best-preserved large mercurian basin. The basin was first imaged in its entirety by the Mercury Dual Imaging System (MDIS) onboard the MErcury Surface, Space ENvironment, GEochemistry, and Ranging (MESSENGER) spacecraft, during its first flyby. Imaging showed the basin to be filled with a large expanse of smooth volcanic plains, like much of the northern latitudes of Mercury [1,4]. Post-impact modification has also resulted in some parts of Caloris' interior exceeding its basin rim by 1 km [5,6]. Caloris has two main interior units: low reflectance material (LRM) and high reflectance plains (HRP) [1,2,7]. The volcanic HRP unit covers the majority of the basin floor interior; LRM has been exposed on the basin surface via cratering events. The LRM is thought to be a minimum of 7.5-8.5 km thick [8,9] and may possibly represent basin floor material [9] and, therefore, be lower crustal and/or upper mantle-like in composition.

Here, numerical modeling of the Caloris impact is undertaken to investigate basin formation and structure. Distribution of crustal and mantle material post-impact is analyzed and quantitative values of melt volume and thickness are calculated and used to interpret the origin of the LRM. Transient crater properties are used to explore any effects of the impact on Mercury's large core. Finally, modeling of Caloris will allow insight into basin formation on Mercury, which may be different than basin formation on the Moon [10].

Methods: The iSALE shock physics code [11-13] was used to model Caloris-sized impacts. iSALE has previously been used to study other large-scale impact basins within the Solar System including Chicxulub, Earth [14] and South Pole-Aitken, the Moon [15]. The impacts were modeled into a halfspace target divided into a 50 km thick crust [9,16], on top of a mantle 350 km thick, with an iron core beneath. Semi-analytical equations of state (ANEOS) for basalt [17], dunite [18] and iron [19] were used to represent the mercurian crust, mantle and core, respectively. Dunite was additionally used to represent the impactor which varied in size and velocity from 50-250 km and 15-50 km/s, respectively. Grid cell size was 5 km, comparable to other large-scale basin modeling [15]. Surface gravity was kept constant at 3.7 m/s^2.

Two target thermal profiles, suitable for the time of the Caloris impact [20-22], were investigated. The profiles had gradients of 8 K/km and 15 K/km. Following previous modeling of large basin-scale impacts [15], an effective viscosity of 10^{10} Pa s for partially molten (super solidus) material was included.

Results: Figure 1 illustrates two time steps in a Caloris-sized basin-forming impact. The top panel shows the transient crater (defined as forming once the expanding transient cavity reaches its maximum volume, in line with previous numerical modeling) which reaches this state 4.33 minutes after initial impact. The lower panel shows the basin after dynamic processes have ceased 120 minutes after impact.

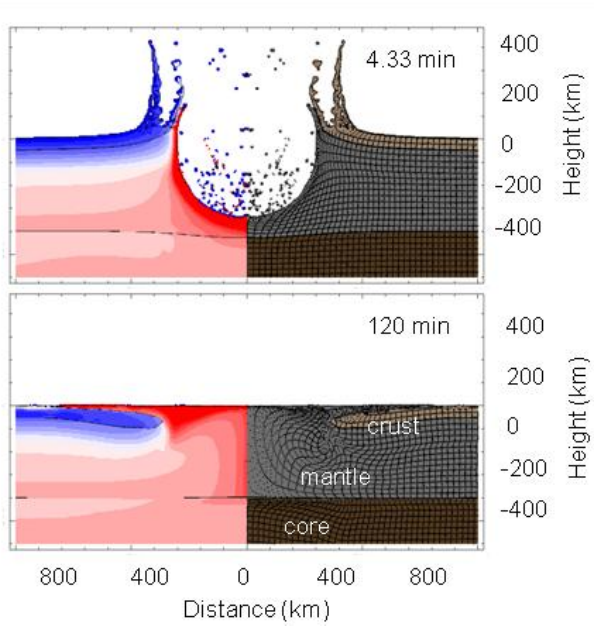

Figure 1: A Caloris-sized impact event showing the transient crater (top) and the final basin (bottom) structure. Left panels show temperature (blue is low, red is high); right panels material (crust, beige; mantle, gray; core, brown). Impactor 100 km diameter, velocity 42 km/s.

Basin size was constrained by the continuous extent of mantle material at the mercurian surface, used here as an analogy for the (possible) extent of LRM. In Figure 1 mantle material extends to a radial distance of ~800 km from the basin center. This surficial material, as well mantle down to the core, is heated to temperatures in excess of the mantle solidus. Melt volumes for impacts of this energy (10^{27} J) are predicted to be on the order of 10^7 km^3 [23].

Figure 2 illustrates excavation depth versus transient crater depth for a number of modeled mercurian basin-forming impacts into a target with a thermal gradient of 8 K/km. The figure shows that excavation depth increases as transient crater size (depth) increases. A range of Caloris-sized basins is highlighted. These particular impacts excavated well into the mantle (i.e., all crustal material was removed from the basin center), but their transient craters did not penetrate to Mercury's core. To produce the Caloris-sized basin shown in Figure 1, material was displaced from a depth of 340 km and excavated from a (maximum) depth of 82 km.

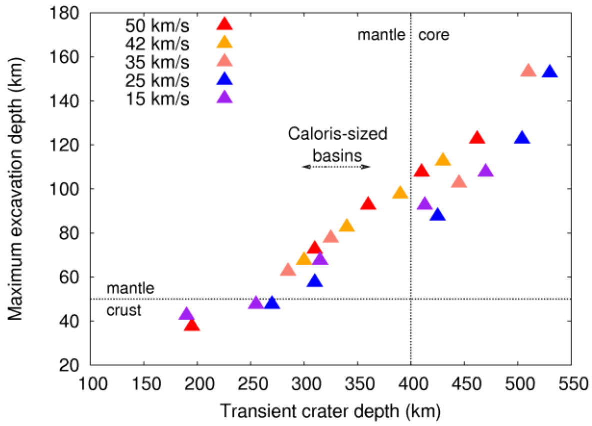

Figure 2: Excavation depth against transient crater depth for a suite of mercurian basin-forming impacts. Results show Caloris-sized basins will excavate mantle material, but the transient crater will not penetrate into the core.

Discussion: [8] suggested Caloris' transient crater had a diameter of 730 km diameter and excavated from a depth of 73 km. This work, however, suggests a slightly smaller transient crater (~600 km diameter) but a ~14% greater excavation depth. This difference is likely due to the initial thermal conditions; a given transient crater will produce a relatively larger final crater if the impact occurs into a warm target [24].

The Caloris impact could have melted material to a depth of 220 km and formed a melt layer 3-15 km thick [9], which could account for the thickness of the LRM. This work suggests melting to a greater depth. The melt volume also implies differentiation of this material, where a new low(er) density, crustal-like layer replaces the initially mantle-rich material towards the surface [25,26]; the crustal thickness beneath Caloris today is ~10-20 km [16]. This work suggests the LRM could well be differentiated mantle material. Further analysis is needed, however, to fully quantify the melt extent and volume in the models, and its relationship to the LRM. The mercurian basin, Rembrandt, displays low-albedo material, similar to the LRM, that has also been interpreted as impact melt [27,28].

These preliminary models suggest the Caloris-forming impact: (1) had an energy on the order of 10^{27} J; (2) excavated mantle material, but (3) did not penetrate to Mercury's core. Due to the size of Caloris relative to Mercury's radius, impacts into a spherical target will also be investigated as curvature could affect transient crater size and ejecta distribution. Results here suggest that the initial dynamic phase of basin formation on Mercury is comparable to that on the Moon. Greater degradation of mercurian basins relative to their lunar counterparts [10], therefore, appears to be due to post-dynamic processes (e.g., basin relaxation, volcanism).

Acknowledgments: We thank iSALE developers Gareth Collins, Boris Ivanov, Jay Melosh, Kai Wünnemann and Dirk Elbeshausen.

References: [1] Murchie, S. L. et al. (2008) *Science*, 321, 73-76. [2] Fassett, C. I. et al. (2009) *EPSL*, 285, 297-308. [3] Marchi, S. et al. (2013) *Nature*, 499, 59-61. [4] Head, J. W. et al. (2011) *Science*, 333, 1853-1856. [5] Obserst, J. F. et al. (2010) *Icarus*, 209, 230-238. [6] Zuber, M. T. et al. (2012) *Science*, 336, 217-220. [7] Robinson, M. S., et al. (2008) *Science*, 321, 66-69. [8] Ernst, C. M. et al. (2010) *Icarus*, 209, 210-223. [9] Ernst, C. M. et al. (in press) *Icarus*, doi: 10.1016/j.icarus.2014.11.03. [10] Fassett, C. I. et al. (2012) *JGR*, 117, E00L08. [11] Amsden, A. A. et al. (1980) Los Alamos National Laboratory Report LA-8095. [12] Collins, G. S. et al. (2004) *MAPS*, 39, 217-231. [13] Wünnemann, K. et al. (2006) *Icarus*, 180, 514-527. [14] Collins, G. S. et al. (2002) *Icarus*, 157, 24-33. [15] Potter, R. W. K. et al. (2012) *Icarus*, 220, 730-741. [16] Smith, D. E. et al. (2012) *Science*, 336, 214-217. [17] Pierazzo, E. et al. (2005) *GSA Spec. Pap.* 384, 443-457. [18] Benz, W. et al. (1989) *Icarus*, 81, 113-131. [19] Thompson, S. L. and Lauson, H. S. (1972) Sandia National Laboratory Report SC-RR-71 0714. [20] Hauck, S. A. et al. (2004) *EPSL*, 222, 713-728. [21] Zuber, M. T. et al. (2010) *Icarus*, 209, 247-255. [22] Roberts, J. H. and Barnouin, O. S. (2012) *JGR*, 117, E02007. [23] Abramov, O. et al. (2013) *Icarus*, 218, 906-916. [24] Potter, R. W. K. et al. (2015) *LPSC XLVI*, #1952. [25] Vaughan, W. M. et al (2013) *Icarus*, 223, 744-765. [26] Vaughan, W. M. and Head, J. W. (2014) *PSS*, 91, 101-106. [27] Whitten, J. L. and Head, J. W. (submitted) *Icarus*. [28] Whitten, J. L. et al. (2014) *LPSC XLV*, #1289.